Improving the Short-Circuit Reliability in IGBTs

How to Mitigate Oscillations

Reigosa, Paula Diaz; Iannuzzo, Francesco; Rahimo, Munaf; Corvasce, Chiara; Blaabjerg, Frede

Published in:
I E E E Transactions on Power Electronics

DOI (link to publication from Publisher):
10.1109/TPEL.2017.2783044

Publication date:
2018

Document Version
Accepted author manuscript, peer reviewed version

Improving the Short-Circuit Reliability in IGBTs: How to Mitigate Oscillations

Díaz Reigosa, Paula; Iannuzzo, Francesco; Rahimo, Munaf; Corvasce, Chiara

Published in:
IEEE Transactions on Power Electronics

DOI (link to publication from Publisher):
10.1109/TPEL.2017.2783044

Publication date:
Dec. 2017

Improving the Short-Circuit Reliability in IGBTs: How to Mitigate Oscillations

Paula Diaz Reigosa, *Student Member, IEEE,* Francesco Iannuzzo, *Member, IEEE,* Munaf Rahimo, *Member, IEEE,* Chiara Corvasce, and Frede Blaabjerg, *Fellow, IEEE*

***Abstract*—In this paper, the oscillation mechanism limiting the ruggedness of IGBTs is investigated through both circuit and device analysis. The work presented here is based on a time-domain approach for two different IGBT cell structures (i.e., trench-gate and planar), illustrating the 2-D effects during one oscillation cycle. It has been found that the gate capacitance varies according with the strength of the electric field near the emitter, which in turn leads to charge-storage effects associated with low carrier velocity. For the first time, it has been discovered that a parametric oscillation takes place during the short-circuit in IGBTs, whose time-varying element is the Miller capacitance, which is involved in the amplification mechanism. This hypothesis has been validated through simulations and its mitigation is possible by increasing the electric field at the emitter of the IGBT with the purpose of counteracting the Kirk Effect.**

***Index Terms*—Insulated gate bipolar transistor, short circuit, gate oscillations, parametric oscillation, robustness, Kirk Effect, TCAD.**

I. Introduction

The Insulated-Gate Bipolar Transistor (IGBT) has firmly established itself in high-voltage and high-current applications, handling power outputs ranging from a few kW to several MW in the power electronics industry [1]. Despite of its great success, many challenges are ahead to meet the future high-reliability targets, in response to the ever increasing demands for more renewable energy applications. For instance, it has been said that the IGBT is one of the critical components according to a survey based on field experiences from power electronics manufacturers [2]. To improve the IGBT reliability and guarantee e.g. 20 years operation, such as in the case of renewable energy systems [3], random failures as the ones occurring during short-circuit conditions cannot be neglected. One of the failures often observed in IGBTs is related to a ringing phenomenon occurring under short-circuit events. Examples of failures caused by oscillations can be found for a trench IGBT power module in [4] and for a trench IGBT chip in Fig. 1. As shown in Fig. 1, a 3.3-kV trench IGBT chip is tested under two DC-link voltages of 1,200 V and 1,500 V, showing low and high frequency oscillations. According to the literature [4], [5], high-frequency oscillations are the precursor or a sign of IGBT failure and this has also being confirmed through experiments (see the experimental result in Fig. 1 at 1,500 V DC-link voltage).

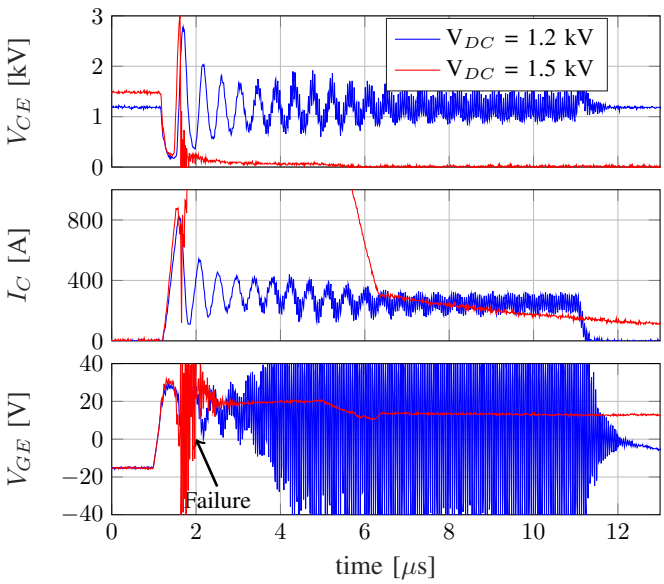

Fig. 1. Short-circuit failure of a 3.3-kV trench IGBT chip tested under two DC-link voltages of 1,200 V and 1,500 V at room temperature: V_{CE} - collector-emitter voltage, I_C - collector current and V_{GE} - gate-emitter voltage.

The oscillation mechanism has been studied over the years [6], [7] showing that, under adverse combinations of large circuit stray inductance under certain operating conditions, it is likely that IGBTs exhibit high-frequency oscillations. Several experimental evidence of such phenomenon can be found in [6], [8]–[11] and, recently, also for trench-gate, field-stop IGBTs [4], [5], [12], [13]. So far, two different approaches have been followed to cope with the oscillations: circuit analysis and device analysis. The first one is related to those theories claiming that the oscillations can be solved by optimizing the external circuit parameters, for instance, by increasing the gate resistance [14], minimizing the stray inductances [8], or proposing stability criteria to avoid the unstable regions [10]. On the other hand, different studies claim that the IGBT chip itself presents some kind of instability. However, different interpretations have been given: the presence of a negative capacitance under high temperatures and high collector voltages [6], the lack of optimization of the IGBT cell design [8] and the dynamic IMPact ionization Avalanche Transit Time (IMPATT) effect [9]. It is clear that

Manuscript received June 06, 2017; revised October 23, 2017, accepted Nov 30, 2017. Recommended for publication by Associate Editor

P.D. Reigosa (*Corresponding Author*), F. Ianuuzzo and F. Blaabjerg are with the Department of Energy Technology, Aalborg University, DK-9220, Denmark, e-mail: (pdr@et.aau.dk)

M. Rahimo and C. Corvasce are with Research and Development, ABB Ltd. Semiconductors, CH-5600 Lenzburg, Switzerland

the above works provide an extensive experimental characterization of the ringing phenomenon, but there has not been a conclusive theory to explain the root cause of such an amplifying behaviour. But what is even more important is that such oscillations still compromise today's IGBT reliability [15].

The purpose of this investigation is to understand the complex behaviour of the IGBT with both circuit and device analysis, as presented in [16], e.g. for the diode snappy recovery. This approach is adopted in this work to find the interaction between the capacitive behaviour of the IGBT and the main circuit parameters. To that end, a trench-gate and a planar-gate IGBT structures have been simulated under short circuit in order to reproduce the gate-voltage oscillations. The results reveal that the oscillation mechanism does not depend on the cell structure type (i.e., planar or trench) but on the IGBT inherent characteristics. IGBTs have pretty low n-base doping and high-level carrier injection features, which favours the Kirk effect occurrence.

This paper is organized as follows: Section II presents the description of the considered IGBT structures. Section III and IV demonstrate the oscillation phenomenon via experimental tests and TCAD simulations, respectively. Section V proposes the root cause of such oscillations along with a simulation model. Section VI proposes a possible device solution by adopting a modification in the IGBT design. Finally, concluding remarks are given.

II. Device Structure

Fig. 2 shows the two IGBT cell designs adopted, whose blocking capability is 3.3-kV: the Soft-Punch-Through (SPT) IGBT with a planar cell (Fig. 2a), and the Soft-Punch-Through (SPT) IGBT with a trench cell and additional carrier enhancement at the emitter (Fig. 2b) [17]. The two IGBT cells are based on the SPT concept having the same buffer design and drift region thickness. On the other hand, the carrier profile distribution of each device is slightly different. The planar IGBT has been designed with a weaker anode (i.e., lower anode injection efficiency) in contrast with the trench IGBT. This, in turn, leads to a lower carrier concentration at the collector, and therefore, smaller turn-off losses. On the other hand, the trench IGBT cell enhances the carrier concentration at the emitter side of the IGBT by introducing an n^+ layer surrounding the p-well layer [18]. As a result, the conduction losses in the trench IGBT are smaller in comparison with the planar IGBT. Moreover, a floating p^+ layer has been implemented in the region between adjacent active cells in the trench device. In this way, the gate input capacitance can be effectively reduced, while also providing an optimum blocking capability [19].

In this work, a traditional planar IGBT without carrier enhancement technology and better anode engineering, and then a state-of-the-art trench IGBT design with carrier enhancement technology and reduced Miller capacitance are compared with focus on the short-circuit oscillations. Both technologies are used to verify the proposed interpretation.

III. Experimental Results

This section presents the experimental results on the short-circuit capability of both planar and trench Soft Punch Through (SPT) IGBTs rated at 3.3-kV. The measurements have been done on a single-chip IGBT soldered on an Alluminium Nitride (AlN) substrate. A non-destructive short-circuit tester consisting of a high voltage power supply with a maximum voltage of 6.5 kV has been used, which is connected to a bank of capacitors. Two IGBT sub-modules act as circuit breaker and the busbar stray inductance can be modified with different inductor values up to a maximum of 2 μH. A Personal Computer (PC) serves as an interface between a 500 MS/s, 500 MHz LeCroy LT344 oscilloscope and the two gate driving units for device under test and series protection. The platform to program the short-circuit sequence and to analyse the data is based on the Laboratory Virtual Instrument Engineering Workbench, provided by the LabVIEW software [20].

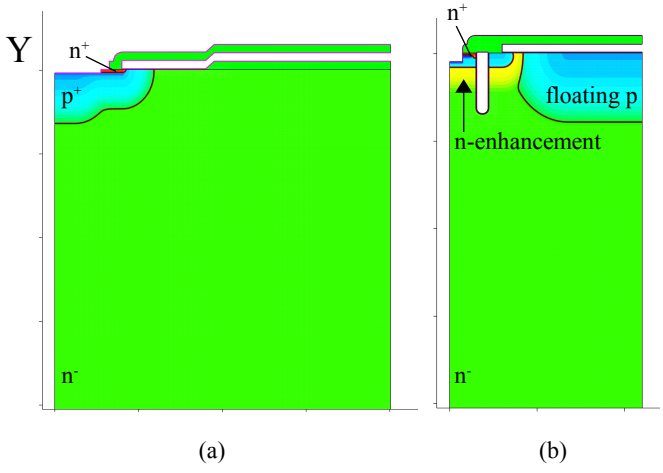

Fig. 2. The 3.3-kV planar IGBT (a) and the 3.3-kV enhanced-trench IGBT (b). The emitter side is only represented for showing the differences between the planar and trench gate structures.

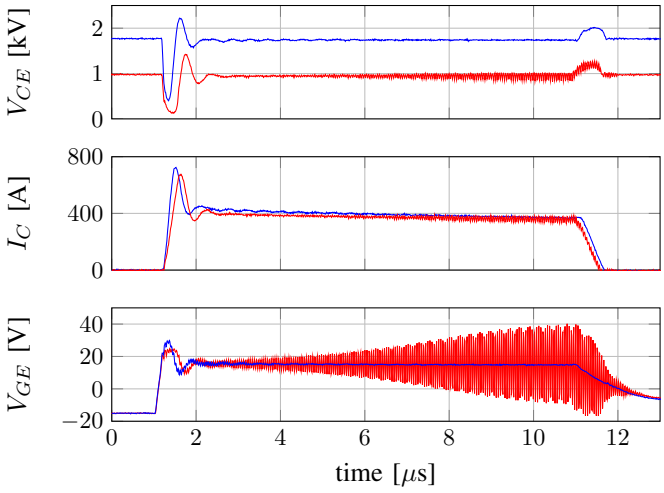

Fig. 3. Short-circuit test of a Soft-Punch Through (SPT) 3.3-kV planar IGBT at different DC-link voltages of 1 kV (red) and 1.9 kV (blue) (T = 25°C, $R_{g,on}$ = 2.2 Ω and L_σ = 580 nH.)

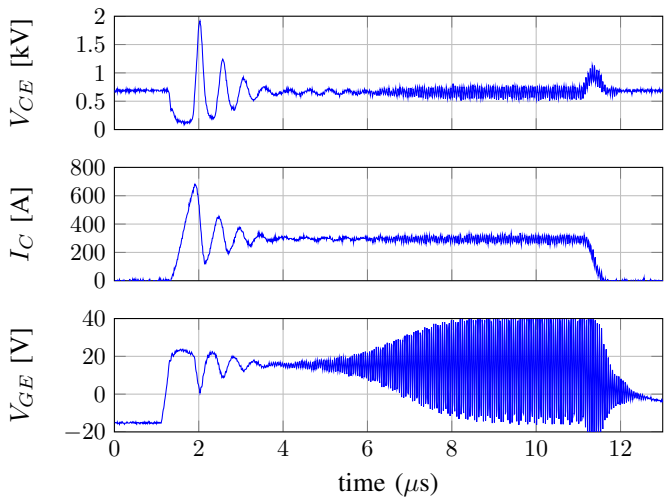

Fig. 4. Short-circuit experiment of a Soft-Punch Through (SPT) 3.3-kV trench IGBT at 700 V DC-link voltage (T = 25°C, $R_{g,on}$ = 2.2 Ω and L_σ = 580 nH.)

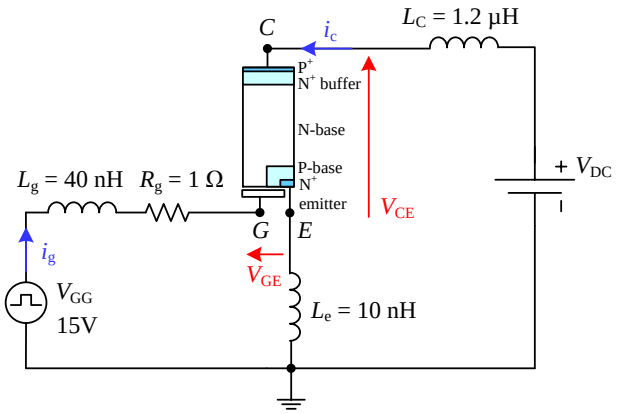

Fig. 5. Circuit used to perform the mixed-mode device simulations with Sentaurus TCAD simulator.

Fig. 3 shows the typical short-circuit type 1 experiment [21] of a 3.3-kV planar IGBT tested under two DC-link voltages of 1 kV and 1.9 kV. While gate oscillations are observed at 1 kV DC-link voltage, the oscillations disappear at higher DC-link voltages (i.e., 1.9 kV). The amplitude of the oscillation rapidly increases in a few microseconds for both gate and collector voltage waveforms. The oscillation frequency of the gate and collector waveforms are in the same range, being 20.8 MHz. The driving factors for the occurrence of the short-circuit oscillations have been previously investigated by the authors in [4], [7], [12], [22] and by others in [21], through the variation of the operating conditions, such as DC-link voltage, gate-emitter voltage and temperature. Particularly in [4], it has been pointed out that the oscillation frequency increases with the applied DC-link voltage, meaning that the Miller capacitance is involved in the oscillation phenomenon. This interpretation is confirmed later in this article.

Similarly, the 3.3-kV trench IGBT has been tested with a low DC-link voltage of 700 V. Fig. 4 demonstrates that the trench IGBT device also shows oscillations with a frequency of 20 MHz. The situation is even more critical since the gate oscillation amplitude is larger in comparison with the experiments on the planar IGBT chip. Nevertheless, this oscillation has a zero damping characteristic, which means that the oscillation is sustained and the IGBT successfully passes the short-circuit condition. On the contrary, in Fig. 1, the failure of the IGBT is unavoidable since the oscillation grows without bound.

IV. TCAD Simulations during Short Circuit

A. The turn-on process under a short circuit

Finite-element device simulations have been performed by means of Sentaurus TCAD simulator [23], in order to understand the physical behaviour of both planar and trench IGBTs during a short-circuit type 1 turn-on process. Simulations have been carried out including the external circuit of Fig. 5, whose values are taken from the experimental circuit but also favoring the occurrence of the oscillation phenomenon. The collector inductance has been selected to have a large value of 1.2 μH, which is realistic in case of motor drive and other applications because of long cables. The gate parameters have been measured within the same frequency range as the oscillations, however, the input impedance during short-circuit has not been measured, as presented in [11]. The main reason is because this paper is not intended to provide a stability map of the IGBT where a combination of parameters may move the IGBT into an unstable region. Instead, the root cause of oscillations will be explained from the device physics perspective, based on a time-domain approach. Additionally, the experimental results in Fig. 3 point out that the high-frequency oscillations are not observed at high DC-link voltages. To that end, a high DC-link voltage level of 2 kV is selected, with the purpose of firstly analyze a clean short-circuit turn-on process without oscillations.

Fig. 6a shows the simulated current and voltage waveforms of the planar IGBT during its turn-on process under a short-circuit type 1, while Fig. 6b indicates the electric field variation and electron carrier distribution associated to the time instants in Fig. 6a. The cuts have been done in the vertical direction through the maximum current density region of the IGBT. The simulations show that during short-circuit, the IGBT builds up a dense electron carrier density near the emitter, while the excess electron charge density in the collector of the IGBT is slightly smaller. The importance of this charge carrier distribution is reflected on the electric field shape whose peak gradually transfers from the emitter side to the collector side, which is commonly known as the Kirk effect. Basically, the amount of electrons prevails over the sum of holes and the background concentration, therefore, the effective charge N_{eff} in the drift region becomes negative (N_{eff} = N_D + h - e).

Fig. 7a shows the simulated electrical waveforms of the trench IGBT during its turn-on process under a short-circuit condition, while Fig. 7b indicates the electric field variation and electron carrier distribution associated to the time instants in Fig. 7a. Once again, the electron carrier density near the emitter becomes pretty dense during the short-circuit condition. Therefore, the electric field peak located at the emitter

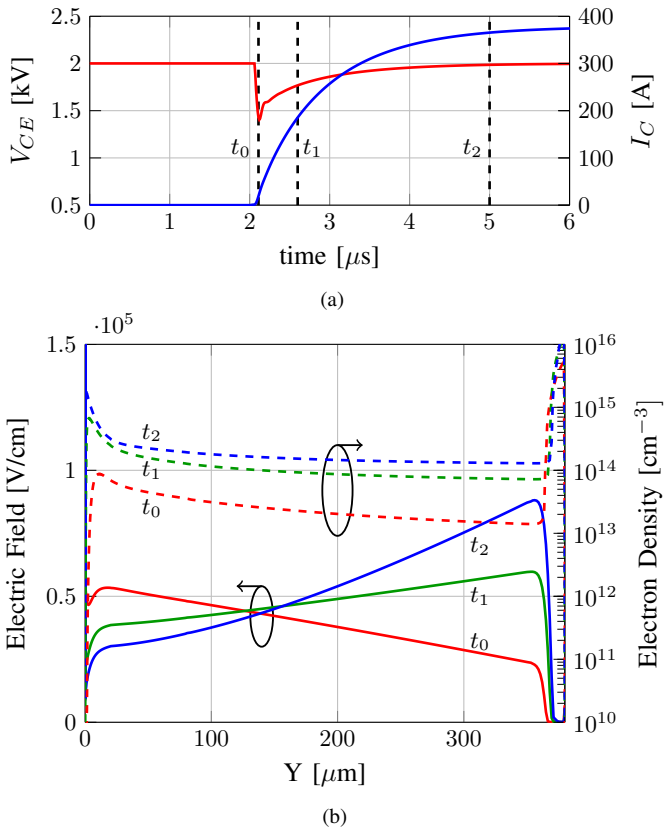

Fig. 6. Short-circuit characteristic of the SPT 3.3-kV planar IGBT: (a) the voltage and current waveforms and (b) the electron carrier distribution and electric field variation associated with the highlighted time instants.

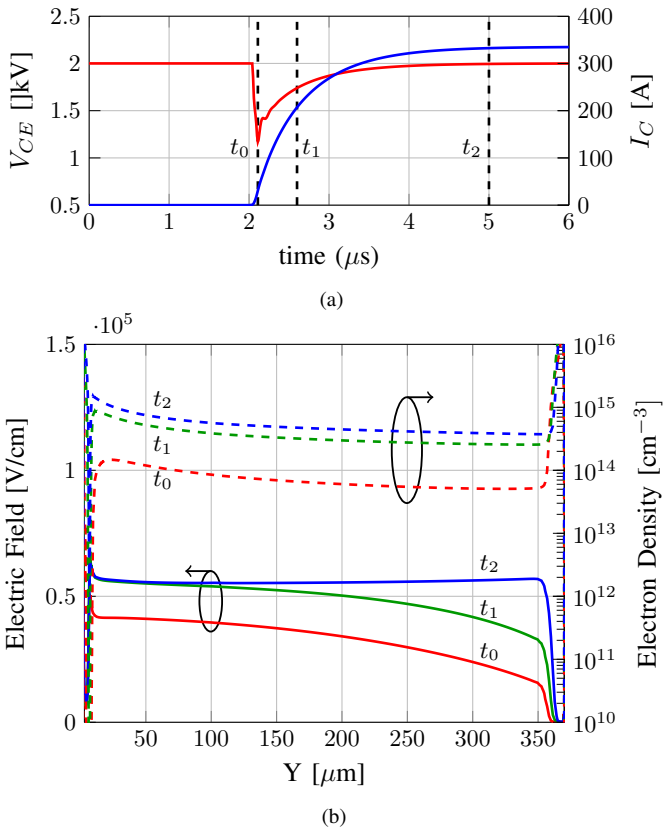

Fig. 7. Short-circuit characteristic of the SPT 3.3-kV trench IGBT: (a) the voltage and current waveforms and (b) the electron carrier distribution and electric field variation associated with the highlighted time instants.

gradually transfers to the collector, as the collector voltage across the IGBT increases. However, for the trench IGBT, the rotated-field is not as pronounced as in the case for the planar IGBT. It is worth to note that the trench design having a higher emitter efficiency shows the benefit of minimizing the drawback coming from the Kirk effect, i.e., the electric field rotates later with time.

B. Analysis of the Short Circuit Oscillations

The short-circuit capability of the IGBT has been demonstrated to be limited by high-frequency oscillations, which may turn into a loss of control and consequent failure. To analyze the physical mechanisms taking place during the short-circuit oscillations, mixed-mode device simulations have been carried out with the set of parameters presented in Fig. 5. The main difference from previous simulations is that a lower DC-link voltage has been applied, therefore, the oscillations can now be observed. Figs. 8 and 9 demonstrate that the oscillation phenomenon can also be reproduced via mixed-mode device simulations for both planar and trench IGBT cells. This is of particular importance in order to identify which parameters influence the short-circuit process and later justify the root cause of such oscillations.

From the experimental and simulation results, it can be assumed that the collector current remains constant, as a 2% and 10% maximum variation is observed, respectively. The oscillation characteristic for both planar and trench IGBT cells

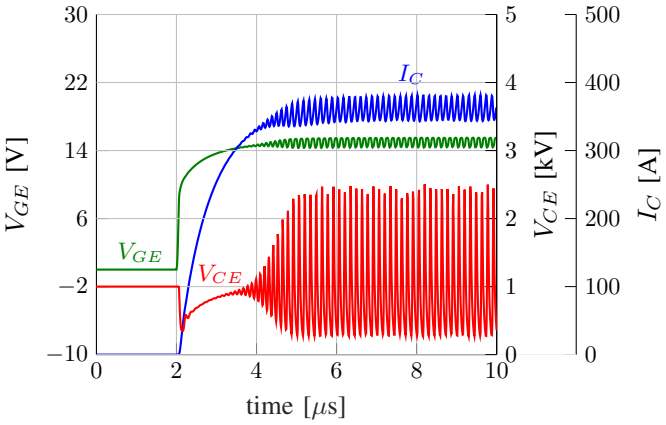

Fig. 8. Short-circuit simulation of an SPT 3.3-kV planar IGBT at V_{DC} = 1 kV showing oscillations during the turn-on process.

look very similar to each other. Therefore, a time-zoom of the oscillations from the planar IGBT (see Fig. 10) is enough to show the phase-shift relation between each electrical parameter (i.e., V_{CE}, I_C, I_g and V_{GE}). In this graph, the gate current and instantaneous input capacitance are added with respect to Fig. 8 for a clearer understanding. In Fig. 10, it can be observed that the gate current i_g is leading the gate voltage V_{GE} by 90°, therefore, it can be assumed that the circuit is nearly capacitive. The instantaneous input capacitance is calculated from i_g and V_{GE} through the formula, $C_i = i_g \times dt/dV_{GE}$. During one

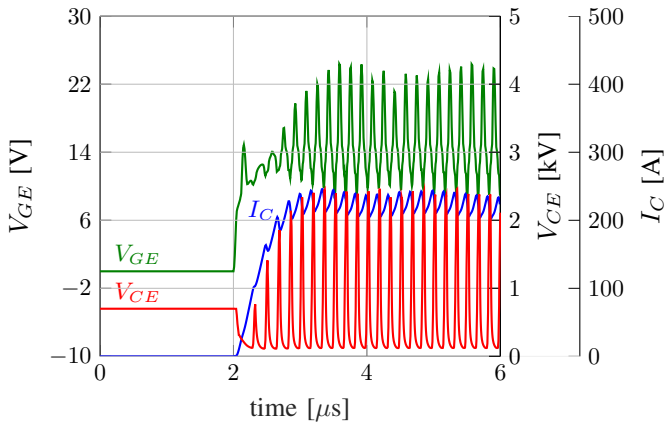

Fig. 9. Short-circuit simulation of an SPT 3.3-kV enhanced-trench IGBT at V_{DC} = 700 V showing oscillations during the turn-on process.

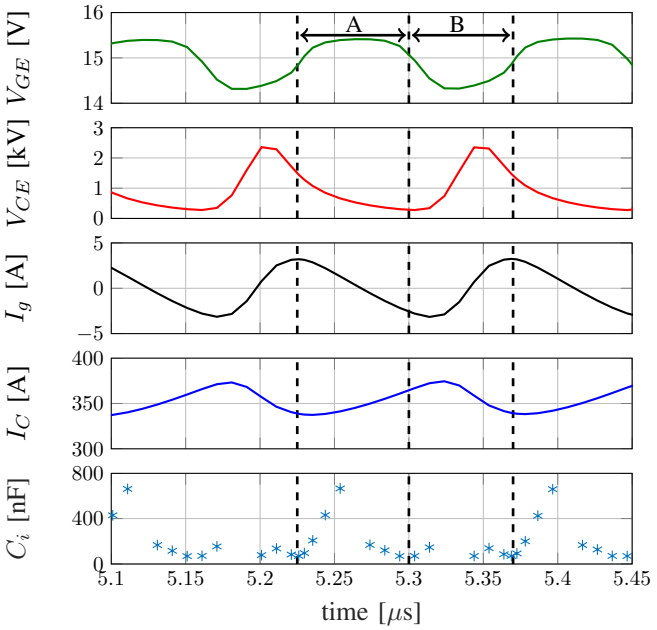

Fig. 10. Time-zoom of Fig. 8 showing the two phases (A and B) taking place during one oscillation cycle, together with the corresponding instantaneous gate capacitance C_i.

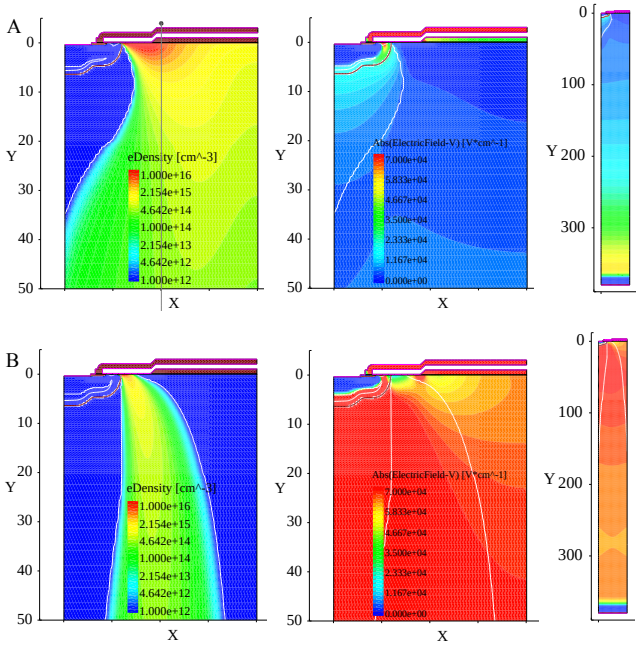

Fig. 11. The SPT 3.3-kV planar IGBT during phases A and B from top to bottom. Left: electron density; middle: electric field; right: electric field through the whole cell. The cut line for Fig. 12 is highlighted.

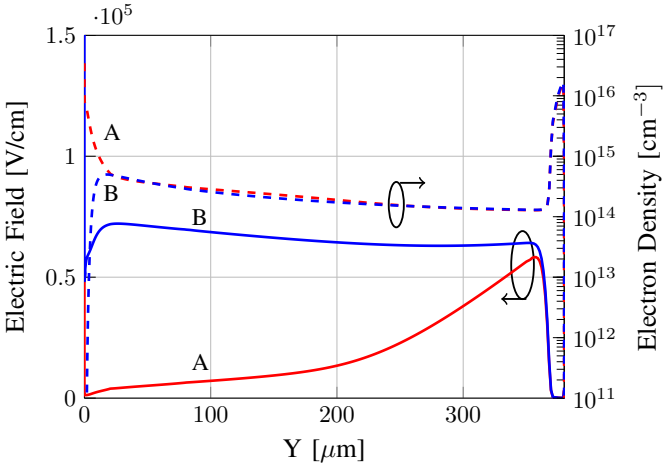

Fig. 12. Simulated electric field (solid line) and electron carrier concentration (dashed line) for the planar IGBT during phases A and B along a cut in the vertical direction (see Fig. 11).

oscillation cycle, it can be observed that the IGBT exhibits a large variation of the input capacitance, which comes from the distribution of the stored excess carriers inside the IGBT, as it will be explained later. To reach a firm conclusion, one oscillation cycle is divided into two phases (see Fig. 10): phase A (charge-storage phase) and phase B (voltage build-up phase); in this way a detailed description can be given for each phase.

1) Phase A: Charge-Storage Phase: During this phase, a carrier accumulation region appears at the surface of the IGBT coinciding with an increase of the input capacitance, about 10 times higher, as it is calculated in Fig. 10. The gate voltage V_{GE} takes higher values than 15 V, which in turn causes the collector voltage V_{CE} to drop in order to sustain the assumed constant collector current. The electron accumulation effect is observed as soon as V_{CE} drops, which is associated with a decrease in the electric field function. In short-circuit conditions, the electric field has been found to be weaker at the emitter of the IGBT, therefore, the carriers move slower in this region. The observed charge-storage effect is in agreement with the assumption of constant collector current, $J_n = qnv_n$, implying that a lower electron velocity can only result in a higher electron density driving the IGBT into the Kirk Effect mode. This behaviour is confirmed in Figs. 11 and 13 for both planar and trench cells, where a low electric field at the emitter coincides with electron accumulation effects.

From the external circuit point of view, the gate current waveform in Fig. 10 indicates that two mechanisms take place: (i) *a charge period (positive i_g)*: the gate capacitance has a

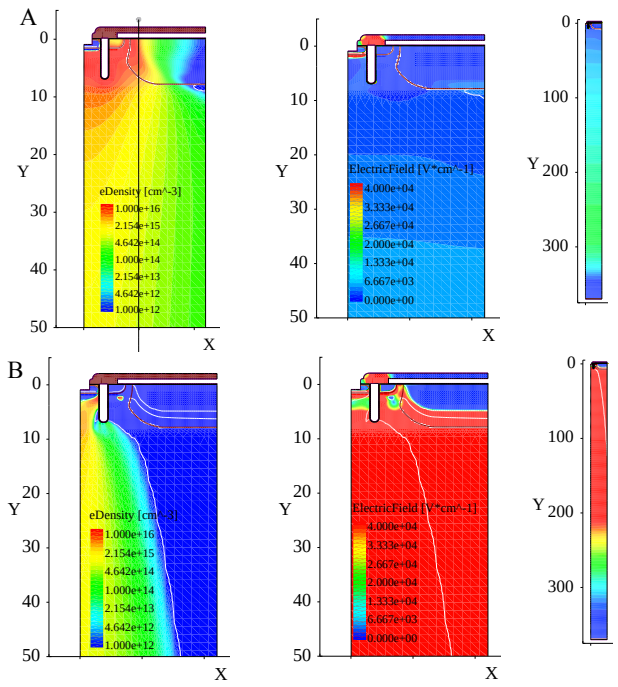

Fig. 13. The 3.3-kV enhanced-trench IGBT during phases A and B from top to bottom. Left: electron density; middle: electric field; right: electric field through the whole cell. The cut line for Fig. 14 is highlighted.

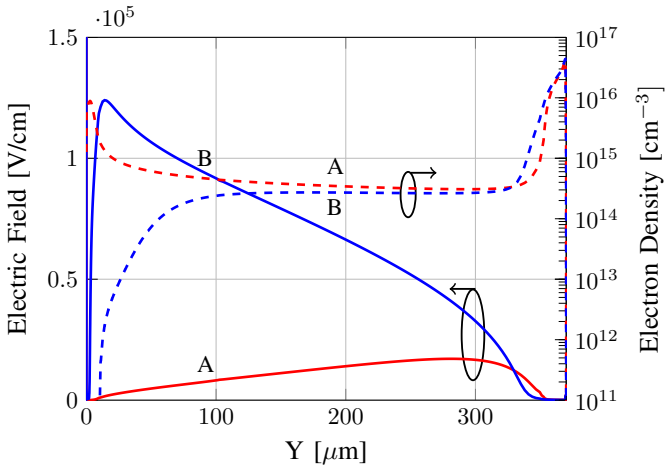

Fig. 14. Simulated electric field and electron carrier concentration for the trench IGBT during phases A and B along a cut in the vertical direction (see Fig. 13).

large value when the capacitor is charged up, so the energy initially stored in the gate inductance is now transferred to a larger gate capacitance. The dV_{GE}/dt slows down because the capacitance is increased. Once the current reaches zero, the capacitance is charged beyond the gate driver voltage (V_{GG} = 15V in Fig. 5) and it starts discharging, reversing the current through the inductance; (ii) *a discharge period (negative i_g)*: the voltage across the large capacitance starts falling as the current through the gate inductance begins to rise. Therefore, the energy stored in the capacitor is now transferred to the inductance. During this transition, the gate capacitance changes its value from a high to a low value causing a larger V_{GE} decrease.

2) Phase B: Voltage Build-Up Phase: During this phase, the electron accumulation region at the surface of the IGBT disappears coinciding with a smaller value of input capacitance. The excess carrier concentration near the emitter is swept out as soon as the collector voltage V_{CE} rises for sustaining the collector current at a lower gate-emitter voltage. Because of higher V_{CE}, the electric field builds-up across the n-base of the IGBT, which in turn implies an increase in the electron velocity. A higher electron velocity is associated with a reduction in the electron density and thus the Kirk Effect is counteracted. As a consequence, the rotated electric field comes back to its well-known triangular shape. This is confirmed in Figs. 11 and 13 for both planar and trench devices. By looking at the gate current, the input capacitance charges and discharges during phase B, but now the capacitance has a small value. It is also worth to look energy-wise at the proposed mechanism. In particular, the time instant when an energy increment occurs is when the surface is flooded with carriers because of Kirk effect. At that time, the collector current leaks some charge at high voltage. Such a charge is returned back to the main collector flow at low voltage, ending up in a net energy transfer from the power loop circuit (DC) to the oscillation (AC).

In summary, the evolution of the IGBT during the short-circuit oscillations varies between two situations which are represented in Fig. 15: (a) a rotated-field associated with electron accumulation effects (i.e., high capacitance) at the

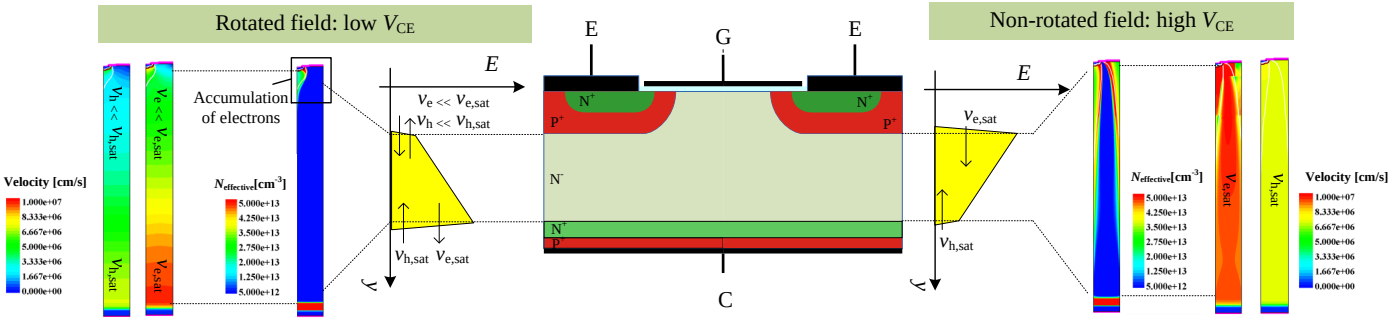

Fig. 15. The internal physical mechanisms of the IGBT under short-circuit oscillations for high and low V_{CE}: v_e - electron velocity, v_h - hole velocity, $N_{effective}$ - effective charge concentration, E - electric field, and $v_{e,sat}$, $v_{h,sat}$ - electron and hole saturation velocities.

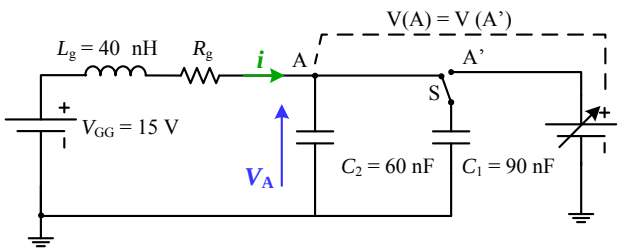

Fig. 16. PSpice simulation circuit using one fixed capacitance (C_2) and a switched one ($C_1 + C_2$) mimicking the capacitance increase to model the amplification behaviour observed in IGBTs during short circuit: S - switch.

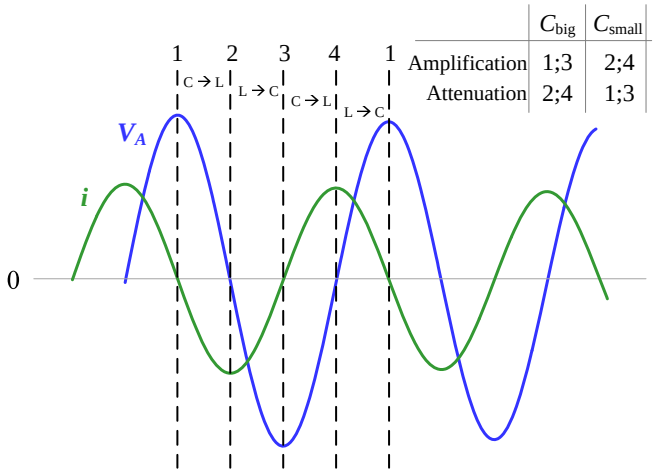

Fig. 17. Current and voltage waveforms of a typical LC circuit showing the time instants at which the capacitors need to be changed: $C_{big} = C_1 + C_2$ and $C_{small} = C_2$.

emitter of the IGBT, due to low carrier velocities at low V_{CE}. This is observed during phase A in Figs. 12 and 14 for planar and trench cells, and (b) a non-rotated field associated with holes prevailing over electrons moving at their saturated values (i.e., low capacitance) due to high V_{CE}. This is observed during phase B in Figs. 12 and 14 for both planar and trench cells. As a consequence of this mechanism, the IGBT presents a time-varying gate capacitance change according to the electric field shape and position of the excess carriers. This is in fact the basis of a parametric oscillation, where the capacitor behaves as an active element. This concept is elaborated in the following.

V. Parametric Oscillations in IGBTs

The results from the mixed-mode simulations have demonstrated that during the oscillations, the instantaneous input capacitance behaves as a time-varying element. The fluctuation of the non-linear Miller capacitance together with the series connected gate resonance circuit gives rise to an energy transfer between the IGBTs input capacitance and the gate inductance L_g. The amplification behaviour arises from the capacitance variation in time. Even if the IGBT acts as an amplifier at the oscillation frequency of 20 MHz [11], the observed oscillations are not caused by the IGBT's gain, as proved later by simulations. This type of amplification has been studied in other fields, and it is commonly recognized as a parametric oscillation; similar to the operating principle of a varactor parametric oscillator, whose non-linear variable capacitor element is used to amplify [24].

The non-linear equations describing the IGBT model together with the external circuit take a complex form. On the other hand, the interpretation of such an amplifying phenomenon is more obvious through simulations. To validate the proposed hypothesis, a PSpice simulation has been built in order to justify how oscillations can diverge or being self-sustained with time. Fig. 16 shows the schematic circuit representing the gate circuit loop consisting of resistive/inductive elements connected in series with two capacitors that are switched alternatively to obtain different effective capacitances. One fixed capacitor represents the small value (C_2), and a switched one, mimics the capacitance increase, in case of charge accumulation (C_1 + C_2). The voltage across the two capacitances is ensured to be the same with the regulated voltage supply (V(A) = V(A$'$)). The gate inductance value has been selected in agreement with the value from the TCAD simulation (i.e., 40 nH), a small resistor is included to simulate circuit losses and the values of the two capacitances have been selected one 50% larger than the other. The value of the gate resistance plays an important role to dampen the oscillations, but it should be large enough to dissipate the energy increase that it is being transferred back and forth between L_g and C. The collector inductance L_C is excluded in this simulation because the collector current I_C remains practically unchanged. However, L_C affects the IGBT short-circuit process in three ways [22]: (1) with higher collector inductance L_C, an increased undershoot across the collector-emitter voltage is observed (this effect is disadvantageous since the electric field becomes weaker and thus the charge accumulates at the surface of the IGBT); (2) the oscillation frequency increases with decreasing L_C and (3) the oscillation amplitude remains constant, meaning that L_C variations do not contribute to the amplification.

The time instants at which the capacitors need to be changed are very crucial to have an amplification or attenuation of the signal. The graph in Fig. 17, representing the current and voltage waveforms of an LC circuit, will help to explain the concept. During one oscillation period, there are four energy transfers between the inductor and the capacitor, represented in Fig. 17 as L $\rightarrow$ C and C $\rightarrow$ L. At the time instants 1 and 3, the current in the circuit is zero, this means that no energy is stored in the inductor and the capacitance is fully charged. On the contrary, at the time instants 2 and 4, the current reaches its maximum value, thus, the energy is stored in the inductance and the capacitance is totally discharged. To obtain the maximum energy increase in the circuit, the capacitance has to vary from a small to a big value at the time instants 1 and/or 3, and change back to a small value at the time instants 2 and/or 4. It is particularly important that the capacitance has a large value when all or most of the total energy is stored in the capacitance (i.e., time instants 1 and 3). Thus, later in time, when all the energy is stored in the inductance and the

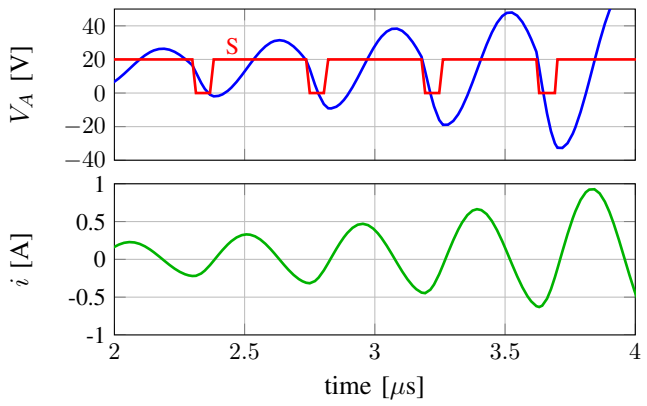

Fig. 18. Simulation of oscillations diverging with time. The switch S is multiplied by 20, which represents the change between the low (S=0) and high capacitance (S=1).

capacitance is switched to a small value (i.e., time instants 2 and 4), the voltage signal will be amplified because the same energy has to be stored in a smaller capacitance.

With the aim of reproducing the same capacitance variation, as the one observed with the device simulations in Fig. 10, the small and large capacitance values are selected at the time instants 2 and 3, respectively. The use of a variable capacitance that reacts non-linearly with the mentioned time sequence is highly effective, as it is shown in Fig. 18. The current i and the voltage V_A are shown, as well as the function S that represents the switching between the low and high capacitance values, where the higher value of S corresponds with the large capacitance (i.e., C_1 + C_2).

In sum, in the TCAD simulations, the capacitance varies as a result of the electric field variation and charge profile distribution; in the PSpice simulation the capacitance variation is controlled with a voltage supply, i.e., switch S in Fig. 18. The transition from low to high capacitance is done when the energy is being transferred from the capacitance to the inductance. This, in turn, causes the dV_A/dt to slow down because the capacitance increases; this is in agreement with the results from the TCAD simulation. On the other hand, the transition from high to low capacitance is done when the energy is transferred back to the capacitance, thus the voltage V_A increases its amplitude because a higher energy has to be stored in a smaller capacitance.

VI. Perspective Solution: Surface Buffer Layer

The primary cause for the electron carrier accumulation at the emitter of the IGBT is the weak electric field in this region, as a consequence of the Kirk effect. The carrier distribution can be adjusted by inserting an n-doped buffer layer at the surface of the IGBT. In this way, the background doping concentration at the emitter is increased, counteracting the negative effective charge. The surface buffer layer has been effectively employed in the 3.3-kV planar IGBT. Fig. 19 shows a comparison between the standard planar IGBT and the proposed one through a short-circuit simulation carried out at the same conditions and with the same stray elements. It is demonstrated that the oscillation phenomenon has been eliminated with the additional surface n-layer. However, when the n-layer is employed, the blocking capability of the IGBT is reduced. Therefore, the n-layer doping concentration must be optimized to achieve the desired carrier distribution near the emitter without substantially reducing the breakdown voltage of the IGBT.

Fig. 20 shows a cut along the vertical direction, just before the oscillations are observed for the standard IGBT at t = 3μs (see Fig. 19). The graph compares the simulated electric field and electron carrier concentration for both standard and proposed IGBTs. A higher electric field is built up at the pn-junction on the emitter side reducing the carrier density. The most important aspect is that the electric field does not strongly depend on the injected carriers and therefore it does not vary with increasing short-circuit time (i.e., the capacitance becomes fixed).

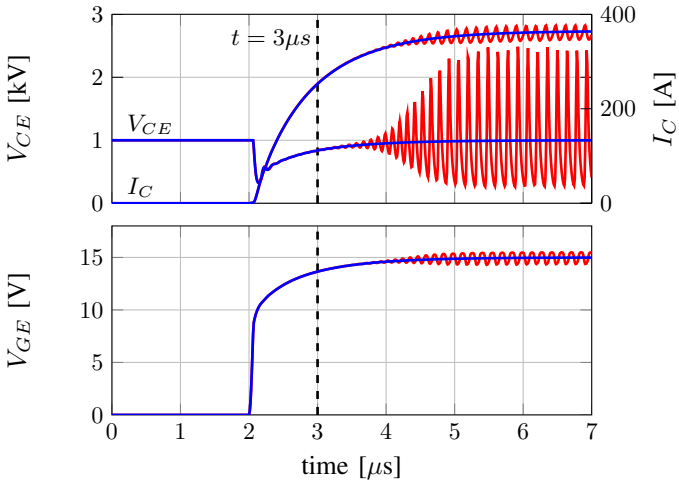

Fig. 19. Short-circuit simulations of an SPT 3.3-kV planar IGBT at 1 kV DC-link voltage demonstrating that the oscillation phenomenon can be mitigated: standard IGBT (red curves) and surface-buffer layer IGBT (blue curves).

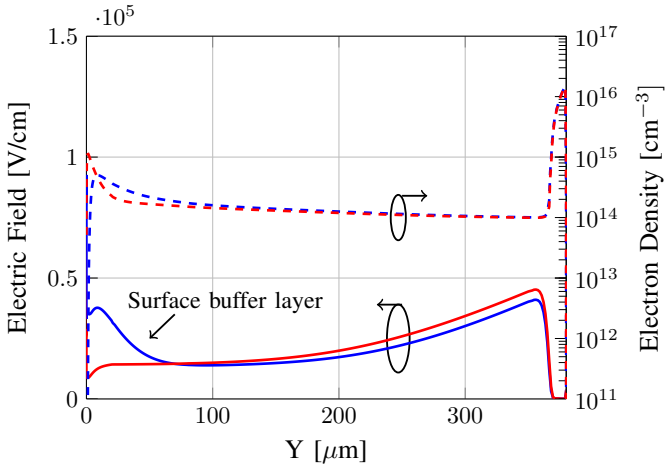

Fig. 20. Simulated electric field (solid line) and electron carrier concentration (dashed line) along a cut in the vertical direction at the time instant highlighted in Fig. 19: standard IGBT (red curves) and surface-buffer layer IGBT (blue curves).

VII. Conclusions

A detailed study of the short-circuit behavior in IGBTs points out that a parametric oscillation takes place in the IGBT. The analysis has demonstrated that the electric field peak across the n-base is continuously changing from the emitter to the collector side coinciding with a high capacitance value when the electric field peak is located at the collector and with a low capacitance value when the electric field peaks at the emitter. The increase of gate capacitance has been correlated with charge-storage effects occurring at the surface of the IGBT at relatively low collector voltages. This hypothesis is coherent with experimental observations at higher voltages, where oscillations are not further observed. The amplification mechanism has been modeled in PSpice with the help of two capacitors (one higher than the other), which are switched alternatively together with an RLC resonant circuit, showing the typical behavior of parametric oscillators. Finally, a mitigation proposal by inserting an n-doped layer at the surface of the IGBT is given. The adoption of an n-doped surface-buffer layer has proven to be effective in IGBTs for bringing about the desired increase in the electric field at the emitter, which prevents Miller capacitance variations.

Acknowledgment

The authors would like to thank ABB Switzerland Ltd. Semiconductors, Lenzburg, Switzerland for sharing a realistic planar and trench IGBT models for Finite-Element Simulations with TCAD and their helpful discussions.

References

[1] M. Rahimo, "Future trends in high-power bipolar metal-oxide semiconductor controlled power semi-conductors," *Circuits, devices and systems*, vol. 8, no. 3, pp. 155–167, 2014.

[2] S. Yang, A. Bryant, P. Mawby, D. Xiang, L. Ran, and P. Tavner, "An industry-based survey of reliability in power electronic converters," *IEEE Transactions on Industry Applications*, vol. 47, no. 3, pp. 1441–1451, May 2011.

[3] H. Wang, M. Liserre, F. Blaabjerg, P. de Place Rimmen, J. B. Jacobsen, T. Kvisgaard, and J. Landkildehus, "Transitioning to physics-of-failure as a reliability driver in power electronics," *Journal of Emerging and Selected Topics in Power Electronics*, vol. 2, no. 1, pp. 97–114, March 2014.

[4] P. Reigosa, R. Wu, F. Iannuzzo, and F. Blaabjerg, "Robustness of MW-Level IGBT modules against gate oscillations under short circuit events," *Microelectronics Reliability*, vol. 55, no. 9-10, pp. 1950–1955, Aug. 2015.

[5] K. Saito, T. Miyoshi, D. Kawase, S. Hayakawa, T. Masuda, and Y. Sasajima, "Suppression of self-excited oscillation for common package of Si-IGBT and SiC-MOS," in *Proc. of the 29th International Symposium on Power Semiconductor Devices and IC's (ISPSD)*, May 2017, pp. 427–430.

[6] I. Omura, W. Fichtner, and H. Ohashi, "Oscillation effects in IGBT's related to negative capacitance phenomena," *IEEE Transactions on Electron Devices*, vol. 46, no. 1, pp. 237–244, Jan 1999.

[7] P. D. Reigosa, F. Iannuzzo, and M. Rahimo, "TCAD analysis of short-circuit oscillations in IGBTs," in *Proc. of the 29th International Symposium on Power Semiconductor Devices and IC's (ISPSD)*, May 2017, pp. 151–154.

[8] M. Takei, Y. Minoya, N. Kumagai, and K. Sakurai, "Analysis of IPM current oscillation under short circuit condition," in *Proc. of the 10th International Symposium on Power Semiconductor Devices and ICs.*, Jun 1998, pp. 89–93.

[9] S. Fujita, K. H. Hussein, S. Kitamura, and T. Yamaguchi, "Investigation on IGBT high-frequency plasma extraction transient time oscillation," *IEEE Transactions on Power Electronics*, vol. 24, no. 6, pp. 1570–1576, June 2009.

[10] C. Abbate, G. Busatto, A. Sanseverino, F. Velardi, and C. Ronsisvalle, "Analysis of low- and high-frequency oscillations in IGBTs during turn-on short circuit," *IEEE Transactions on Electron Devices*, vol. 62, no. 9, pp. 2952–2958, Sept 2015.

[11] C. Abbate, G. Busatto, A. Sanseverino, F. Velardi, S. Iavarone, and C. Ronsisvalle, "Measurement of IGBT high-frequency input impedance in short circuit," *IEEE Transactions on Power Electronics*, vol. 32, no. 1, pp. 584–592, Jan 2017.

[12] P. D. Reigosa, R. Wu, F. Iannuzzo, and F. Blaabjerg, "Evidence of gate voltage oscillations during short circuit of commercial 1.7 kV/1 kA IGBT Power Modules," in *Proc. of PCIM Europe 2015*, May 2015, pp. 1–8.

[13] R. Wu, P. D. Reigosa, F. Iannuzzo, L. Smirnova, H. Wang, and F. Blaabjerg, "Study on oscillations during short circuit of mw-scale IGBT power modules by means of a 6-kA/1.1-kV nondestructive testing system," *Journal of Emerging and Selected Topics in Power Electronics*, vol. 3, no. 3, pp. 756–765, Sept 2015.

[14] K. Mochizuki and Y. Tomomatsu, "IGBT module," Patent US 20 050 194 660, Sept. 08, 2005.

[15] J. Lutz, U. Scheuermann, H. Schlangenotto, and R. D. Doncker, *Semiconductor Power Devices: Physics, Characteristics, Reliability*. New York, NY, USA, Springer-Verlag, 2011.

[16] M. T. Rahimo and N. Y. A. Shammas, "Freewheeling diode reverse-recovery failure modes in IGBT applications," *IEEE Transactions on Industry Applications*, vol. 37, no. 2, pp. 661–670, Mar 2001.

[17] A. Kopta, M. Rahimo, C. Corvasce, M. Andenna, F. Dugal, F. Fischer, S. Hartmann, and A. Baschnagel, "Next generation IGBT and package technologies for high voltage applications," *IEEE Transactions on Electron Devices*, vol. 64, no. 3, pp. 753–759, March 2017.

[18] M. Rahimo, A. Kopta, and S. Linder, "Novel enhanced-planar IGBT technology rated up to 6.5 kV for lower losses and higher SOA capability," in *Proc. of the International Symposium on Power Semiconductor Devices and IC's*, June 2006, pp. 1–4.

[19] C. Corvasce, M. Andenna, S. Matthias, L. Storasta, A. Kopta, M. Rahimo, L. De-Michielis, S. Geissmann, and R. Schnell, "3300V HiPak2 modules with Enhanced Trench (TSPT+) IGBTs and Field Charge Extraction Diodes rated up to 1800A," in *Proc. of the PCIM*, May 2016, pp. 1–8.

[20] "LabVIEW," http://www.ni.com/en-us/shop/labview.html.

[21] A. Volke and M. Hornkamp, *IGBT Modules*. Infineon Technologies AG, Second edition, 2012.

[22] P. D. Reigosa, F. Iannuzzo, and F. Blaabjerg, "Packaging solutions for mitigating IGBT short-circuit instabilities," in *Proc. of the International Exhibition and Conference for Power Electronics, Intelligent Motion, Renewable Energy and Energy Management (PCIM)*, May 2017, pp. 1–7.

[23] "Sentaurus-device Technology Computer Aided Design TCAD," http://www.synopsys.com.

[24] J. Hilibrand, C. W. Mueller, C. F. Stocker, and R. D. Gold, "Semiconductor parametric diodes in microwave computers," *IRE Transactions on Electronic Computers*, vol. EC-8, no. 3, pp. 287–297, 1959.

Paula Diaz Reigosa (S'14) received the B.S. degree in industrial engineering with a specialization in electrical engineering from the University of Oviedo, Spain, in 2012, and the M.S. degree in power electronics and drives from Aalborg University, Denmark, in 2014. She received the Ph.D. degree in Reliability of Power Electronics from Aalborg University, Denmark, in 2017. She was an intern master student in the Department of Wind Power Systems in Siemens, Aalborg, Denmark, from June to September 2013 and with the Department of Reliability of Power Electronics in Danfoss, Graasten, Denmark, from September 2013 to January 2014. She was a Visiting Ph.D. student with ABB Switzerland Ltd Semiconductors, Lenzburg, Switzerland, in 2016. Her current research interests include the reliability of power devices and especially power device failures, development of non-destructive testing facilities for assessment of high power modules under extreme conditions and emerging power electronics applications.

Francesco Iannuzzo (M'04 - SM'12) received the M.Sc. degree in Electronic Engineering and the Ph.D. degree in Electronic and Information Engineering from the University of Naples, Italy, in 1997 and 2001, respectively. He is primarily specialized in power device modelling. From 2000 to 2006, he has been a Researcher with the University of Cassino, Italy, where he became Aggregate Professor in 2006 and he is currently Associate Professor since 2012. In 2014 he got a contract as professor in Reliable Power Electronics at the Aalborg University, Denmark, where he is also part of CORPE (Center of Reliable Power Electronics). His research interests are in the field of reliability of power devices, including cosmic rays, power device failure modelling and testing of power modules up to MW-scale under extreme conditions, like overvoltage, overcurrent, overtemperature and short circuit. He is author or co-author of more than 120 publications on journals and international conferences and one patent. Besides publication activity, over the past years he has been invited for several technical seminars about reliability in first conferences as EPE, ECCE and APEC.

Munaf Rahimo (M'98) received his B.Sc. from Baghdad University, Iraq in 1991 and his M.Sc. and Ph.D. from Staffordshire University, UK in 1993 and 1996, respectively. He joined the power device R&D department at GEC Plessey Semiconductors, UK in 1996 and in 1998 he joined the power development group at Semelab plc, UK as a senior R&D engineer. He joined ABB Switzerland, Semiconductors in 2000 and has been involved in the R&D of power semiconductor devices for high voltage power electronics applications. Since 2012, he is a Corporate Executive Engineer at ABB Switzerland, Grid Integration. He has worked with many device concepts such as MOSFETs, Diodes, IGBTs, IGCTs, Thyristors and Silicon Carbide based power devices. He pioneered the first high power Reverse Conducting RC-IGBT targeting mainstream hard switching applications. He has 80 patent families and has authored and co-authored 160 conference and journal publications in his field of speciality.

Chiara Corvasce received her M.S. Degree in Physics from the University of Bari, Italy in 1994. In 1995 she joined the Memory Product Group of STMicroelectronics in Catania, working on non-volatile memory devices and leading the team for the development of a ferroelectric memory. In 2002 she has moved to the Integrated Systems Laboratory (IIS) of the ETH Zurich where she received the PhD in Electrical Engineering focusing on high temperature characterization and modeling of semiconductor devices. She joined the BiMOS R&D Department of ABB Semiconductors in 2006 where she has been leading numerous IGBT and diode development projects before she took over the management of the R&D chip development group in 2013. Her main research interest is design and applications of high power semiconductor devices.

Frede Blaabjerg (S'86 - M'88 - SM'97 - F'03) was with ABB-Scandia, Randers, Denmark, from 1987 to 1988. From 1988 to 1992, he was a Ph.D. Student with Aalborg University in Electrical Engineering, Aalborg, Denmark. He became an Assistant Professor in 1992, Associate Professor in 1996, and Full Professor of power electronics and drives in 1998. His current research interests include power electronics and its applications such as in wind turbines, PV systems, reliability, harmonics and adjustable speed drives. He has received 17 IEEE Prize Paper Awards, the IEEE PELS Distinguished Service Award in 2009, the EPE-PEMC Council Award in 2010, the IEEE William E. Newell Power Electronics Award 2014 and the Villum Kann Rasmussen Research Award 2014. He was an Editor-in-Chief of the IEEE TRANSACTIONS ON POWER ELECTRONICS from 2006 to 2012. He is nominated in 2014 and 2015 by Thomson Reuters to be between the most 250 cited researchers in Engineering in the world.